

Fractal nature of chromatin organization in interphase chicken erythrocyte nuclei: DNA structure exhibits biphasic fractal properties

D.V. Lebedev^a, M.V. Filatov^a, A.I. Kuklin^b, A.Kh. Islamov^b, E. Kentzinger^c, R. Pantina^a,
B.P. Toperverg^a, V.V. Isaev-Ivanov^{a,*}

^a Division of Molecular and Radiation Biophysics, Petersburg Nuclear Physics Institute, Russian Academy of Sciences, Gatchina, Russia

^b Frank Laboratory of Neutron Physics, Joint Institute for Nuclear Research, Dubna, Russia

^c Institut für Festkörperforschung, Forschungszentrum Jülich, Jülich, Germany

Received 8 December 2004; revised 29 December 2004; accepted 14 January 2005

Available online 4 February 2005

Edited by Irmgard Sinning

Abstract Arrangement of chromatin in intact chicken erythrocyte nuclei was investigated by small angle neutron scattering. The scattering spectra have revealed that on the scales between 15 nm and 1.5 μm the interior of the nucleus exhibited properties of a mass fractal. The fractal dimension of the protein component of cell nucleus held constant at approximately 2.5, while the DNA organization was biphasic, with the fractal dimension slightly higher than 2 on the scales smaller than 300 nm and approaching 3 on the larger scales.

© 2005 Federation of European Biochemical Societies. Published by Elsevier B.V. All rights reserved.

Keywords: Cell nucleus; Chromatin structure; Small angle neutron scattering

1. Introduction

The current concept for chromatin structure and dynamics in cell nuclei of higher organisms contains two tendencies. On one hand, there are direct experiments showing that the arrangement of chromosomes in interphase nuclei is not random and follow the territorial principle of distribution of genetic material [1]. In this model, the large-scale chromatin structures and the entire chromosomes are fairly stationary. On the other hand, experiments where individual genomic loci were labeled indicate that on the smaller scales (up to 0.5 μm), the chromatin fibre is subjected to random diffusion [2]. Thus, even the large chromatin territories that may appear static and compact formations are subjected to continuous local Brownian motion that makes them permeable to nucleic components with size up to 600 kDa [3].

Based on these evidence one can surmise that in interphase nuclei the large-scale chromatin arrangement is fundamentally different from its small-scale structure. Detecting these differences requires a method that would allow to gather information of the general principles of chromatin organization in

cell nuclei under native or nearly native conditions, but not necessarily with high structural resolution, such as small angle neutron scattering (SANS). Earlier, small angle scattering data of di- and trinucleosomes, solubilized chromatin and cell nuclei [4–6] were obtained in the limited range of scales, in the most part yielding information about low level organization of nucleosomes and chromatin fibers. Modern SANS spectrometers provide an opportunity to measure neutron intensities in the range of scattering vectors between 5×10^{-1} and $7 \times 10^{-5} \text{ \AA}^{-1}$, covering the entire hierarchy of chromatin structures in cell nucleus, from nucleosomal to the nucleus as a whole.

In this work, based on the analysis of SANS on chicken erythrocyte nuclei, we present evidence that both the DNA component and the protein component of chromatin exist in a form of mass fractal and that the DNA component of chromatin exhibits two-phase mass-fractal properties with the crossover length of around 450 nm.

2. Methods

Chicken erythrocytes were obtained from hen blood, which was washed multiple times by centrifugation in isotonic phosphate buffer (pH 7.8) containing 10 mM EDTA to remove blood plasma proteins. Erythrocyte's cytoplasmic membrane was dissolved by non-ionic detergent Triton X-100 (0.2% in phosphate buffer, pH 7.8). Cell nuclei at concentration approximately 10 mg/ml were fixed by 0.05% glutaraldehyde for 10 min and subsequently washed by centrifugation to remove the fixation agent.

Quality and homogeneity of the prepared cell nuclei were controlled by fluorescent flow-cytometry. According to the flow-cytometry data, variation of the DNA content per cell nuclei did not exceed 2%.

Fixed cell nuclei were stored in phosphate buffer at pH 7.4, with 20 mM EDTA added to the buffer to prevent DNA degradation by endonucleases.

For SANS measurements cell nuclei samples were transferred to phosphate buffer containing >99.5% D_2O , incubated for 24 h, centrifuged for 10 min at 3000 RPM and transferred to the fresh D_2O buffer. The procedures for contrast variation measurements were the same, except the appropriate $\text{D}_2\text{O}/\text{H}_2\text{O}$ mixture was used instead of D_2O .

Preliminary SANS data from sedimented nuclei were acquired in the range of $Q = 4\pi/\lambda \sin \theta/2$ from 0.005 to 0.15 \AA^{-1} on JuMO spectrometer [7], located on the 4th channel of the high flux IBR-2 reactor (FLNP JINR, Dubna, Russia). These data exhibited the power law dependency of the scattering intensity vs. the scattering vector in the range of Q from 0.005 to 0.04 \AA^{-1} . Experiment to test the effect of the fixation agent on the scattering spectrum have shown that 10 min treatment with high (1%) concentration of glutaraldehyde (Fig. 1,

*Corresponding author. Fax: +7 81271 32303.

E-mail address: isaev@omrb.pnpi.spb.ru (V.V. Isaev-Ivanov).

Abbreviations: SANS, small angle neutron scattering; FISH, fluorescence in situ hybridization

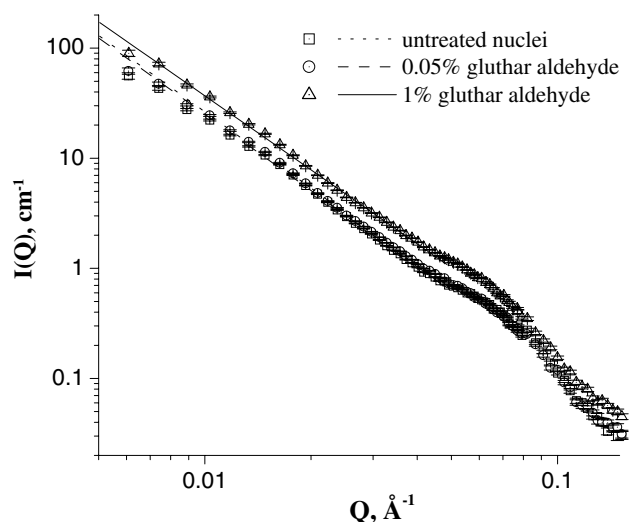


Fig. 1. Small angle neutron scattering spectrum of chicken erythrocyte nuclei in D_2O buffer that were not fixed (squares), fixed with 0.05% (circles) and 1% glutar aldehyde (triangles). Lines represent data fits to the power law in the range from 0.006 to 0.04 \AA^{-1} , with the exponents 2.3 ± 0.02 , 2.3 ± 0.02 and 2.23 ± 0.02 , respectively.

triangles) does not change the overall nature of the scattering curve and has only a slight effect on the power law exponent (that decreased from 2.3 for untreated nuclei to 2.23) and the intensity (likely due to some change of the sedimentation properties of the nuclei). For glutar aldehyde concentration of 0.05%, which was normally used in our preparation procedure, the scattering curves from the freshly made samples of untreated nuclei and from the fixed samples were nearly identical (Fig. 1, squares, circles), indicating that at least on the scales up to several hundreds Å, the chromatin arrangement inside cell nucleus is not affected by our fixation procedure.

To achieve reproducible conditions for the SANS experiments, an agarose matrix was used to suspend cell nuclei for the duration of measurements. Low melting point agarose was dissolved in hot phosphate buffer ($\sim 70^\circ\text{C}$) at 1% concentration, cooled to 50°C and mixed with cell nuclei samples immediately before filling the sample cuvette. Final agarose concentration was 0.7%, nuclei concentrations were set to 10% or 30% by weight. All measurements were performed at room temperature ($17\text{--}22^\circ\text{C}$). Control experiments on JuMO spectrometer did not reveal significant differences in the shape of the scattering curves from sedimented nuclei and from samples suspended in agarose.

SANS measurements with contrast variation in the broad range of scattering vectors (from 10^{-1} to 10^{-4} \AA^{-1}) were performed on KWS-2 and KWS-3 spectrometers at FRJ-2 reactor, Festkörperforschung Institute of the Forschungszentrum Jülich (Germany). Data acquisition on KWS-2 spectrometer was performed at three detector positions, 2, 8 and 20 m, with neutron wavelength set to 8 Å for the first two positions, and 12 Å for the third detector position. KWS-2 data were normalized to the absolute units using scattering from the Lupolen™ standard. KWS-3 data were normalized to fit the KWS-2 data in the region of scattering vectors where the ranges of KWS-2 and KWS-3 spectrometers overlap. For this region, it was possible to linearize the relationship between the scattering intensities and the scattering vectors on a double-logarithmic scale. The KWS-3 data were linearized in the range of $Q = 8 \times 10^{-4}$ – $1.3 \times 10^{-3} \text{ \AA}^{-1}$, while the normalized scattering curve from KWS-2 was linearized in the range of $Q = 1.3 \times 10^{-3}$ – $2.5 \times 10^{-3} \text{ \AA}^{-1}$. The scattering intensity from KWS-3 was multiplied by a constant value to achieve the same absolute intensity for both spectrometers at $Q = 1.3 \times 10^{-3} \text{ \AA}^{-1}$. Contrast variation experiments were performed in phosphate buffer containing 40%, 64% and >99% D_2O . All measurements on KWS-2 and KWS-3 spectrometers were performed with samples suspended in 0.7% agarose matrix. Scattering from the reference sample containing 0.7% agarose matrix and appropriate amount of D_2O was measured for each contrast point and subtracted. All data were normalized to concentration of cell nuclei in the sample, with the concentration of cell nuclei of 30% by weight taken as 1.

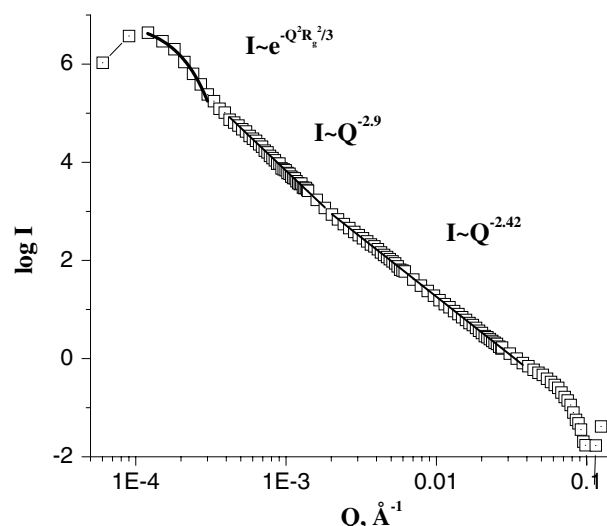


Fig. 2. Small angle neutron scattering spectrum of chicken erythrocyte nuclei suspended in 0.7% agarose gel in D_2O . Scattering by the reference sample, containing the same concentration of agarose in D_2O , was subtracted from the data. Data from both KWS-2 and KWS-3 spectrometers shown on the same plot (see text). Lines represent data fits to the power law with two different exponents and least-square fit to the gaussian in Guinier region below $3 \times 10^{-4} \text{ \AA}^{-1}$.

3. Results

Fig. 2 shows the double-logarithmic plot of the scattering intensities vs. scattering vectors in the combined range of KWS-2 and KWS-3 spectrometers (10^{-1} to 10^{-4} \AA^{-1}). For the sample containing 99% D_2O one can distinguish three regions of the curve:

- (1) In the range of Q from 1.5×10^{-3} to $4 \times 10^{-2} \text{ \AA}^{-1}$, the relationship between the scattering intensity and the scattering vector follows the power law $I \sim Q^{-D}$ and thus can be linearized when plotted on a double-logarithmic scale with the slope of the linear fit $D \sim 2.4$. This result is in agreement with the earlier results obtained on JuMO spectrometer in Dubna [8] and indicates that the structure of chromatin in chicken erythrocyte nuclei on the scale between 15–20 nm and 400 nm exhibits properties that are characteristic of a mass fractal [9].
- (2) For the lower scattering angles, where the values of Q lie between 3×10^{-4} and $1.5 \times 10^{-3} \text{ \AA}^{-1}$, the scattering curve plotted on a double-logarithmic scale is also linear, but the power law exponent changes, so that the slope of the linear fit becomes $D \sim 2.9$. If we stay with the notion that chromatin arrangement possesses mass fractal properties, its fractal dimension approaching the value of 3 implies that increase in the size of the scatterer is no longer accompanied by an increase in the size of the internal density variations in the mass fractal [9]. This range of Q corresponds to the linear dimensions between 400 nm and $1.5\text{--}2 \text{ \mu m}$.
- (3) In the range of scattering vectors $Q < 3 \times 10^{-4} \text{ \AA}^{-1}$ the dependency of the scattering intensity of Q follows the Guinier law. From this dependency we obtain the gyration radius of the scatterers, $R_g = 1.1 \text{ \mu m}$. The calculated value for the gyration radius corresponds to the spherical particle diameter of approximately 3 μm , which is close to the size of the chicken erythrocyte nucleus.

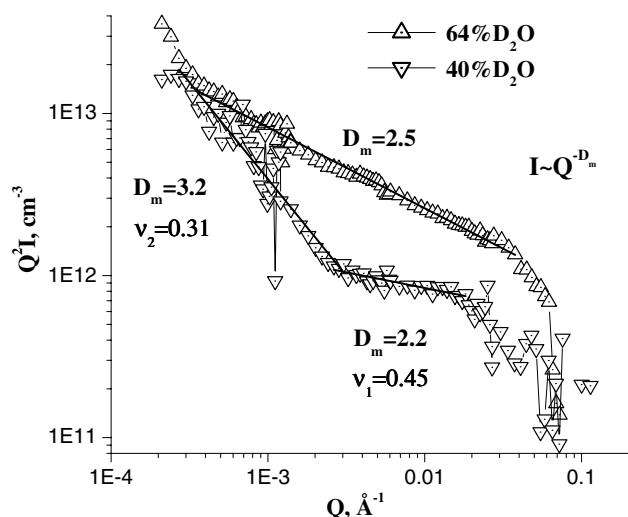


Fig. 3. Small angle neutron scattering by chicken erythrocyte nuclei at two contrast points. Samples were suspended in 0.7% agarose gel, and the scattering by the gel alone was subtracted from the data. Data from both KWS-2 and KWS-3 spectrometers shown on the same plot (see text).

To evaluate the contributions from the protein and the DNA components of chromatin to the scattering intensity of the samples in D_2O , contrast variation measurements were performed on samples containing various ratios of D_2O/H_2O . The results of these measurements are plotted in Fig. 3 using a double-logarithmic Kratky scale ($Q^2 I$ vs. Q).

Fig. 3 shows the scattering curves for samples containing 64% and 40% D_2O , which is near the compensation points for DNA and proteins, respectively. The respective curves can therefore be viewed as the scattering intensities from the protein and the DNA components of chromatin in chicken erythrocyte nuclei. The protein curve exhibits power law behavior of the intensity of scattering over broad range of Q (from 4×10^{-2} to $4 \times 10^{-4} \text{ \AA}^{-1}$) with the exponent $D \sim 2.5$. The curve that corresponds to the DNA component of chromatin has much shorter segment with the power law exponent $D \sim 2.2$ (Q between 2×10^{-2} and $2.5 \times 10^{-3} \text{ \AA}^{-1}$), that at the lower Q changes to the power law dependency with the exponent D of about 3.2 (Q from 2.5×10^{-3} to $3 \times 10^{-4} \text{ \AA}^{-1}$).

These results call for the following conclusions: (i) both the protein component of the chromatin structure and the DNA organization in chicken erythrocyte nuclei exhibit properties of a mass fractal; (ii) protein component of chromatin has a structure that possesses fractal properties on the scales ranging over two orders of magnitude from the size of a nucleosome to the size of an entire nucleus; (iii) DNA arrangement in chicken erythrocyte nucleus is also of a fractal nature and has two levels of organization, or two phases, with the crossover point at around 300–450 nm.

4. Discussion

The fractal nature of chromatin arrangement implies that its structure is irregular on the scales above the size of a nucleosome and has the property of scale-invariance, which in the case of SANS means that the relationship between the size

of the scatterer and the sizes of inhomogeneities within the scatterer remains the same over the entire range of the scattering vectors where the power law determining the fractal properties of the structure applies.

The contrast variation data indicate that the biphasic fractal features seen in the scattering curve from samples in D_2O stem from the two-phase nature of arrangement of the chromatin DNA. The scattering intensity on a randomly oriented mass fractal particle depends on the scattering vector Q as $I(Q) \propto Q^{-D_m}$ where D_m is the dimension of the mass fractal [9]. On the other hand, chain polymer molecules such as chromosomal DNA follow scaling laws [10], which tie the distance between the ends of the polymer chain, R , and the number of the monomers in the chain, N , as $R \propto N^{1/D_c}$, where D_c is the chain dimension. The value $\nu = 1/D_c$ is referred to as Flory exponent [10]. Another law describes the relationship between the mass-dimension of a polymer chain contained in a sphere with the radius of R , with the number of monomers, N , contained in that sphere, as $R \propto N^{1/D_m}$. In the limiting case of $N \rightarrow \infty$ the two dimensions, D_c and D_m , are the same [9]. Applying these relationships to the two-phase experimental curve that reflects scattering by the DNA (40% D_2O), we calculate the Flory exponent $\nu_{Q > Q_k} = 0.45 = \nu_1$ above the crossover point of the curve and $\nu_{Q < Q_k} = 0.31 = \nu_2$ below the point of crossover. According to the Flory theory, the observed value of ν_1 implies that on the scale up to 400 nm the DNA structure resembles Gaussian chain ($\nu_G = 0.5$), with the excluded volume interactions in the chain exhibiting slight prevalence of attraction over repulsion. On the scale above 400 nm the DNA arrangement in chicken erythrocyte nuclei becomes globular, and attractive forces prevail in the volume interactions.

In the earlier works [11,12] folding of chromosomes in human interphase G0/G1 nuclei was investigated by confocal microscopy measurements of the mean distances between fluorescent labels introduced in the DNA using fluorescence in situ hybridization (FISH) technique. Spacing between the sequences labeled by fluorescence ranged between 0.15 and 190 Mbp. The mean square distances between the fluorescent labels were plotted against the length of the DNA sequence between the labeled sites on a double-logarithmic scale [13], revealing two linear regions with the crossover point $S_k \cong 2$ Mbp. The slopes of the lines were $\nu_{S < S_k} = 0.46$ below the crossover point and $\nu_{S > S_k} = 0.32$ above the point of crossover. The mean square distance at the point of crossover, measured by confocal microscope, was $L_k^{\text{FISH}} \cong 1 \text{ \mu m}$.

Thus, both our SANS measurements on chicken erythrocyte nuclei and the above measurements of the mean square distances between fluorescent labels in human chromosomes reveal two phases of the DNA arrangement in cell nuclei. The fractal properties of the DNA structure in each phase, indicated by the corresponding Flory exponent, are very similar for both chicken erythrocyte and human nuclei. The size of the structures at the crossover point is different: for the chicken erythrocyte nuclei $L_k \cong 400 \text{ nm}$, while for the human chromosome $L_k^{\text{FISH}} \cong 1 \text{ \mu m}$. Based of these results, that were obtained by two independent methods, one can suppose that the two-phase fractal nature of the DNA arrangement may be common for cell nuclei of higher organisms.

The crossover point of the fractal structure of DNA seen by SANS is close to the size of clusters observed in studies of DNA replication [14], repair [15] and transcription [16,17] in

cell nuclei. On the scales smaller than the crossover point the structure of DNA resembles that of a random walk polymer, which is characterized by high amplitudes of fluctuations comparable to the size of the entire object. This property of chromatin could also explain local Brownian motion of genomic loci reported earlier and the fact that interphase chromosomes are permeable toward large nucleic components.

The protein component of chromatin exhibits uniform fractal properties on the scales from just above nucleosomal size to nearly the size of the cell nucleus. Interplay between the biphasic fractal organization of the DNA component of chromatin and continuous fractal structure of its protein component calls for further investigation.

Acknowledgements: Authors would like to thank V.A. Nazarenko, RAS corr. member, for his constant attention and support for this work. Financial support for this work came from RAS program “Elementary particle physics” (subprogram “Neutron physics”, direction “Studies of structure, dynamics and non-ordinary properties of matter by neutron methods”), RFBR grant No. 02-04-49259-a and from the grant from Russian Ministry of Science No. 40.012.1.1.1149.

References

- [1] Gerlich, D. and Ellenberg, J. (2003) Dynamics of chromosome positioning during the cell cycle. *Curr. Opin. Cell. Biol.* 15, 664–671.
- [2] Belmont, A. (2003) Dynamics of chromatin, proteins, and bodies within the cell nucleus. *Curr. Opin. Cell. Biol.* 15, 304–310.
- [3] Misteli, T. (2001) Protein dynamics: implications for nuclear architecture and gene expression. *Science* 291, 843–847.
- [4] Notbohm, H. (1986) Small angle scattering of cell nuclei. *Eur. Biophys. J.* 13, 367–372.
- [5] Bordas, J., Perez-Grau, L., Koch, M.H., Vega, M.C. and Nave, C. (1986) The superstructure of chromatin and its condensation mechanism. I. Synchrotron radiation X-ray scattering results. *Eur. Biophys. J.* 13, 157–173.
- [6] Hammermann, M., Toth, K., Rodemer, C., Waldeck, W., May, R.P. and Langowski, J. (2000) Salt-dependent compaction of di- and trinucleosomes studied by small-angle neutron scattering. *Biophys. J.* 79, 584–594.
- [7] Ostanevich, Y.M. (1988) Time-of-flight small-angle scattering spectrometers on pulsed neutron sources. *J. Makromol. Chem. Macromol. Symp.* 15, 91–103.
- [8] Filatov, M.V., Lebedev, D.V., Kuklin, A.I., Islamov, A.K., Lebedev, V.T. and Isaev-Ivanov, V.V. (2002) Small-angle neutron scattering on hen erythrocyte nuclei: fractal nature of DNA arrangement XII International Conference on Small-angle Scattering, p. 26, Venice International University.
- [9] Schmidt, P.W. (1989) Use of Scattering to Determine the Fractal Dimension in: (Avnir, D., Ed.), pp. 67–79, John Wiley & Sons Ltd, New York.
- [10] Elber, R. (1989) Fractal Analysis of Proteins in: *The Fractal Approach to Heterogeneous Chemistry* (Avnir, D., Ed.), pp. 407–423, John Wiley & Sons Ltd, New York.
- [11] Sachs, R.K., van den Engh, G., Trask, B., Yokota, H. and Hearst, J.E. (1995) A random-walk/giant-loop model for interphase chromosomes. *Proc. Natl. Acad. Sci. USA* 92, 2710–2714.
- [12] Yokota, H., van den Engh, G., Hearst, J.E., Sachs, R.K. and Trask, B.J. (1995) Evidence for the organization of chromatin in megabase pair-sized loops arranged along a random walk path in the human G0/G1 interphase nucleus. *J. Cell. Biol.* 130, 1239–1249.
- [13] Munkel, C., Eils, R., Dietzel, S., Zink, D., Mehring, C., Wedemann, G., Cremer, T. and Langowski, J. (1999) Compartmentalization of interphase chromosomes observed in simulation and experiment. *J. Mol. Biol.* 285, 1053–1065.
- [14] Jackson, D.A. and Pombo, A. (1998) Replicon clusters are stable units of chromosome structure: evidence that nuclear organization contributes to the efficient activation and propagation of S phase in human cells. *J. Cell. Biol.* 140, 1285–1295.
- [15] Janicki, S.M. and Spector, D.L. (2003) Nuclear choreography: interpretations from living cells. *Curr. Opin. Cell. Biol.* 15, 149–157.
- [16] Verschure, P.J., van Der Kraan, I., Manders, E.M. and van Driel, R. (1999) Spatial relationship between transcription sites and chromosome territories. *J. Cell. Biol.* 147, 13–24.
- [17] Spector, D.L. (2003) The dynamics of chromosome organization and gene regulation. *Annu. Rev. Biochem.* 72, 573–608.